

THREE-DIMENSIONAL ALIGNMENT AND MERGING OF CONFOCAL MICROSCOPY STACKS

Nisha Ramesh[†] Hideo Otsuna^{*} Tolga Tasdizen[†]

[†] Department of Electrical and Computer Engineering

^{*} Department of Neurobiology & Anatomy
University of Utah, Salt Lake City, Utah, USA

ABSTRACT

We describe an efficient, robust, automated method for image alignment and merging of translated, rotated and flipped confocal microscopy stacks. The samples are captured in both directions (top and bottom) to increase the SNR of the individual slices. We identify the overlapping region of the two stacks by using a variable depth Maximum Intensity Projection (MIP) in the z dimension. For each depth tested, the MIP images gives an estimate of the angle of rotation between the stacks and the shifts in the x and y directions using the Fourier Shift property in 2D. We use the estimated rotation angle, shifts in the x and y direction and align the images in the z direction. A linear blending technique based on a sigmoidal function is used to maximize the information from the stacks and combine them. We get maximum information gain as we combine stacks obtained from both directions.

Index Terms— Confocal Microscopy, Zebrafish, Maximum Intensity Projection, Fourier Shift Theorem.

1. INTRODUCTION

Confocal microscopy is a powerful tool for evaluation of 3D structure of a variety of tissues and biological samples. Biologists analyze small vertebrate models, such as zebrafish because of its similarity to other vertebrates, genetic tractability and optical transparency of its embryo and larvae. The prevalence of confocal imaging has increased rapidly in zebrafish research. One challenge is that the SNR of the slices of the stacks obtained using confocal microscopes decreases with increasing depth. Hence, if we image the organism on the dorsal (back) side we lose partial information from the ventral (front) side of the organism. We generate image stacks from both directions and merge the information from stacks after alignment. The transformation between the dorsal and ventral stacks includes translation in the x , y and z direction, rotation and flipping of the stacks. We get maximum information gain as we combine stacks obtained from both directions. We propose an approach described in section 3 that

computes the unknown 3D translation and rotation between two confocal stacks. We use Maximum Intensity Projection (MIP) of the 3D stacks to roughly estimate the overlap in z . Our method uses the Fourier Shift property in 2D on the MIP images to estimate the rotation angle and the shifts in x and y directions. Finally, the precise shift in the z direction is calculated. The stacks are combined using a linear blending technique based on a sigmoidal function.

2. RELATED WORK

Image alignment is a very important topic in the field of confocal microscopy images. Intensity based registration methods compute transformations using image intensity information [1]. Cross-correlation is a reliable metric for matching directly image intensities between images. Fourier based methods improve the computational speed. The phase correlation registration method is based on the Fourier Shift Theorem [2] and was originally proposed for the registration of translated images. It computes the cross-power spectrum of the target and reference images and looks for the location of the peak in its inverse. The method shows strong robustness against correlated and frequency dependent noise and non-uniform, time varying illumination disturbances. Computational time savings are more significant if the images, which are to be registered, are large. Tasdizen et al. proposed a method to construct large mosaics, align overlapping sections for serial section transmission electron microscopy images [3]. Their method is based on the Fourier shift property to detect the displacement vectors. In their method they align 2D sections to build 3D volume (stack) for serial-section microscopy. In this work, we need to align 3D volumes which are rotated and have unknown number of overlapping slices between the stacks. The method proposed by Preibisch et al. [4] supports confocal stacks in which the only transformation between the stacks is translation. Their method does not support rotation and varying number of overlapping slices between stacks. [5] discusses an extension of the well known phase correlation technique to cover translation, rotation, and scaling. Fourier scaling properties and Fourier rotational properties are used

Supported by NIH grant 1R01-GM098151-01.

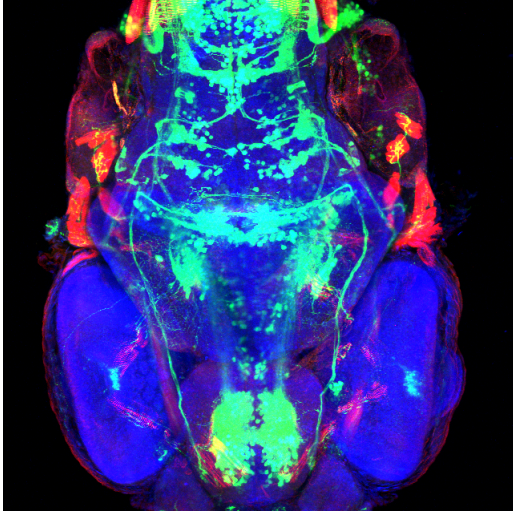


Fig. 1. MIP of dorsal view of brain of Zebrafish

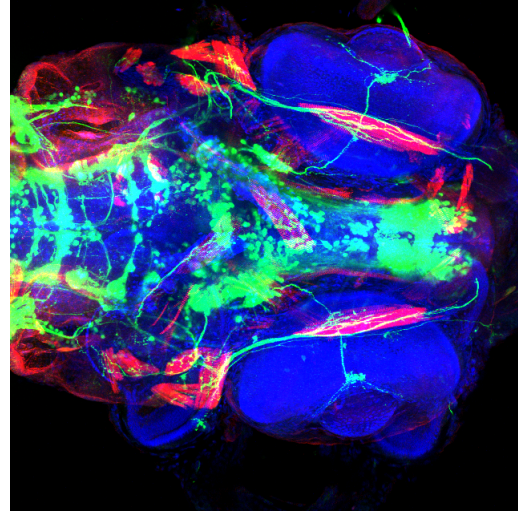


Fig. 2. MIP of ventral view of brain of Zebrafish

to find scale and rotational movement. Another Fourier-based approach that estimates large translations, scalings, and rotation is an algorithm that uses the pseudo polar (PP) Fourier transform to achieve substantial improved approximations of the polar and log-polar Fourier transforms of an image [6]. We will extend similar methods to estimate the rotation in 3D stacks.

3. METHOD

The data consists of dorsal (back) and ventral (front) stacks which need to be aligned and merged with one another. The ventral stack is flipped in the z direction. The MIP of the dorsal and ventral regions are shown in Figure (1) and Figure (2). We use MIP of the 3D stacks to roughly estimate the overlap in z . We vary the number of slices over which the MIP is taken. The Fourier Shift property in 2D on the MIP images is used to estimate the rotation angle and the shifts in x and y directions. Finally, the precise shift in the z direction is calculated for the rotated stacks. The stacks are combined using a linear blending technique based on a sigmoidal function.

3.1. Estimation of overlapping slices in the 3D stack, rotation angle, shift in the x and y direction

We consider the last n slices from one stack (dorsal) and the first n slices from the other stack (ventral). We take the MIP of these n slices for the intensity images. We use the MIP image from one of the stacks as a reference image (dorsal stack). We rotate the MIP image from the other stack in the range of 1 to 360 degrees (increments of 1 degree). For every rotation we estimate the best shift in the x and y direction using 2D Phase Correlation between the reference image and the rotated image.

The Fourier Shift property based phase correlation method [2] is used to compute the translational shifts between the reference and shifted images. This method provides fast computation. Let $F[g](u,v)$ denote the two-dimensional Fourier transform of image $g(x,y)$ where u and v denote the variables in the frequency domain. The cross power spectrum of two images g and h is defined as

$$S(g, h) = \frac{F[g]F^*[h]}{|F[g]F^*[h]|} \quad (1)$$

where F^* denotes the complex conjugate of the Fourier transform. For image g and its circularly shifted version $g_{circ(x_0, y_0)}$ simplifies to $S(g, g_{circ(x_0, y_0)}) = e^{j(ux_0 + vy_0)}$.

The cross power spectrum isolates the complex exponential, the displacement vector (x_0, y_0) can be recovered by taking the inverse Fourier transform of the cross power spectrum (2).

$$C = F^{-1}[S(g, g_{circ(x_0, y_0)})] = \delta(x - x_0, y - y_0), \quad (2)$$

where $\delta(x - x_0, y - y_0)$ is the Dirac delta function located at (x_0, y_0) . In real images, R contains several peaks. We choose the strongest peak by selecting the maximum value of C (3).

$$(x_0, y_0) = \arg \max\{C\} \quad (3)$$

Due to periodicity assumption of the Fourier Transform a peak at (x_0, y_0) can correspond to any one of the four possible displacement vectors (x_0, y_0) , $(Q - x_0, y_0)$, $(x_0, R - y_0)$, $(Q - x_0, R - y_0)$ where (Q, R) is the size of the image. We generate all possible displacements between pair of images, compute the cross correlation of each and choose the displacement vector that yields the best correlation. The cross correlation between images is computed as follows (4)

$$\rho_1 = \frac{\sum_{x,y} (g(x,y) - \mu_g)(g_{circ}(\hat{x}, \hat{y}) - \mu_{g_{circ}})}{\sqrt{(\sum (g(x,y) - \mu_g)^2)(\sum (g_{circ}(\hat{x}, \hat{y}) - \mu_{g_{circ}})^2)}} \quad (4)$$

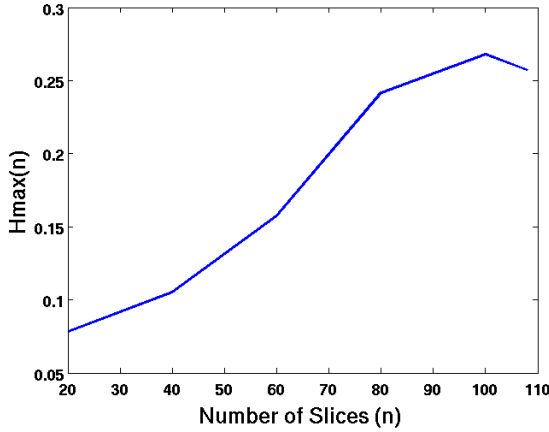


Fig. 3. Hmax(n) vs number of slices (n)

where $\hat{x} = x_0 + x$, $\hat{y} = y_0 + y$.

The cross correlation coefficient represented as H_n between the rotated and shifted image is recorded for every angle of rotation θ , where n signifies the number of slices of overlap. We use the median of the correlation coefficient to help identify significant peaks. The median is denoted as $H_{median.n}$. To check for a strong peak we subtract the median correlation coefficient from the true value.

$$H_n(\theta) = H_n(\theta) - H_{median.n}(\theta) \quad (5)$$

We repeat this step for varying multiples of n till we there is complete overlap between the two stacks. The maximum value of $H_n(\theta) \forall n$ indicates the correct overlap between the stacks, Figure (3), Figure (4). This gives a rough estimate of the overlap in z , denoted as $z_{initial.e}$. The location of the peak helps to determine the angle of rotation between the images. Let θ_e be the estimate of the rotation angle between the dorsal and ventral stacks. We choose the best shift in the x and y direction corresponding to θ_e .

3.2. Image Alignment of the Rotated 3D Stacks

Let θ_e be the estimate of the rotation angle between the dorsal and ventral stacks. Let (x_e, y_e) be the estimates of the shifts in the x and y direction. We first rotate the ventral stack using the estimated angle and translate the slices in accordance with the shifts in the x and y direction. Since we know the rough overlap between the stacks, we limit the shift in the direction to ± 10 of the $z_{initial.e}$ to reduce additional computation. The stacks are denoted as A and B. The cross correlation in 3D between images is computed as follows (6)

$$\rho_2 = \frac{\sum (A(x, y, z) - \mu_A)(B_{\theta_e}(x', y', z) - \mu_{B_{\theta_e}})}{\sqrt{(\sum (A(x, y, z) - \mu_A)^2)(\sum (B_{\theta_e}(x', y', z) - \mu_{B_{\theta_e}})^2)}} \quad (6)$$

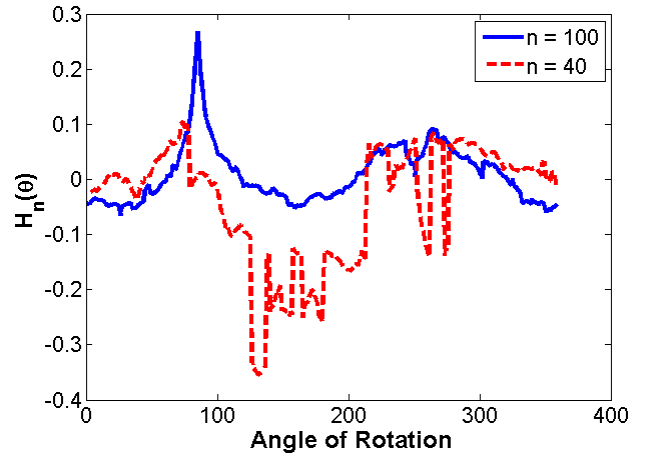


Fig. 4. $H_n(\theta)$ vs angle of rotation (θ), $n = 100$ and $n = 40$

where $x' = x + x_e$, $y' = y + y_e$. The maximum correlation is obtained for the right shift in the z direction.

3.3. Sigmoidal Image Blending

There are visible brightness differences between the slices in the dorsal and the ventral stacks. The dorsal stack has more information in the first half whereas the ventral stack has more information in the latter half. We combine the two stacks by merging the dorsal and ventral stacks. Linear interpolation is used for the overlapping slices. Let $\alpha \in [0,1]$ be the transition parameter. The value of α varies for every overlapping slice in the stack as a sigmoidal function. Let $d_{x,y,z}$ denote a pixel in the first stack (dorsal) and $v_{x,y,z}$ denote a pixel in the second stack (ventral) where $x = 1 \dots Q$, $y = 1 \dots R$, $z =$ any overlapping slice. The result of an image blend is a family of images $w_{x,y,z}$ related using the equation given below (7).

$$w_{i,j,z} = (1 - \alpha(z))d_{i,j,z} + (\alpha(z))v_{i,j,z} \quad (7)$$

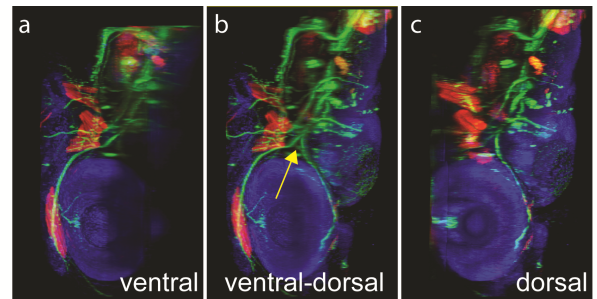


Fig. 5. a) Ventral side data, the dorsal side has no clear signals. c) Dorsal side data, there are no clear neurons on ventral side. b) In our result, the arrow indicates the splitting point for the motor neurons, which projects to ventral and dorsal side of the eye

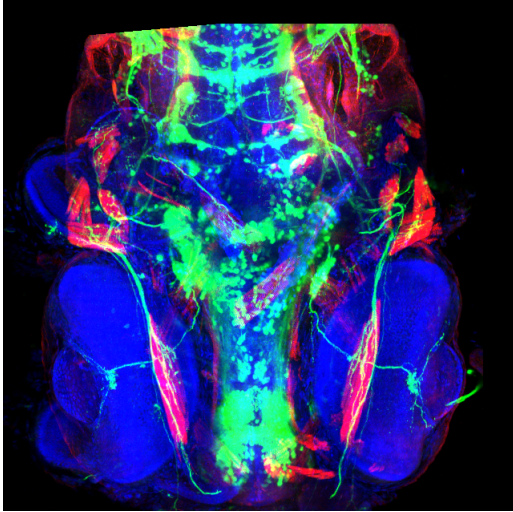


Fig. 6. MIP of ventral view of brain of ZebraFish (after rotation and translation, $x_e = 40$, $y_e = 32$, $\theta_e = 85$)

Table 1. Comparison of estimated shifts with true shifts

DataSet	x_{shift}		y_{shift}		z_{shift}		θ	
	x_e	x_t	y_e	y_t	z_e	z_t	θ_e	θ_t
1	-40	-38	32	32.7	9	9	85	85.2
2	-187	-187	-142	-141	115	115	187	187

4. RESULTS & DISCUSSION

We used our proposed method on two confocal microscopy datasets. The combined image stack from the dorsal and ventral sections show no artifacts from misalignments between the stacks. There is information gain as we combine stacks obtained from both directions as seen is Figure(5). In the ventral side data, the dorsal side has no clear signals, Figure(5a). In the dorsal side data, there are no clear neurons on ventral side, Figure(5c). In our result, the arrow indicates the splitting point for the motor neurons, which projects to ventral and dorsal side of the eye, Figure(5b). We used $n =$ multiples of 20, the number of sections in the MIP to estimate the approximate overlap in the z direction. In the first dataset the correct overlap is close to 100, we see a strong peak in $H_n(\theta)$ for $n = 100$. For incorrect values of n there is no significant peak, Figure(4). The location of the peak determines the angle of rotation between the images. We choose the best shift in the x and y direction corresponding to θ_{est} . The MIP of ventral view of brain of Zebrafish after rotation and translation is shown in Figure(6). The estimated shifts in pixels x_e , y_e , z_e and rotation angle θ_e are compared with the true shifts x_t , y_t , z_t and true rotation angle θ_t in Table (1). The correlation coefficients for the two datasets before and after alignment are shown in Table (2).

This paper presents a methodology to align and combine

Table 2. Comparison of cross correlation results for 3D stacks

DataSet	% overlap slices	Correlation Coeff before alignment	Correlation Coeff after alignment
1	89.25%	0.231	0.7
2	7.25%	0.2128	0.6641

3D confocal microscopy data. This technique is effective in maximizing the information from the two stacks to create a combined stack. Further studies will be focused on using Fourier based methods to estimate the rotation angle in 3D stacks.

5. REFERENCES

- [1] B. Zitova and J. Flusser, "Image registration methods: a survey," *Image and vision computing*, vol. 21, no. 11, pp. 977–1000, 2003.
- [2] Kuglin C.D and Hines D.C, "The phase correlation image alignment method.," in *International Conference on Cybernetics and Society*.
- [3] Tolga Tasdizen, Pavel Koshevoy, Bradley C. Grimm, James R. Anderson, Bryan W. Jones, Carl B. Watt, Ross T. Whitaker, and Robert E. Marc, "Automatic mosaicking and volume assembly for high-throughput serial-section transmission electron microscopy," *Journal of Neuroscience Methods*, vol. 193, no. 1, pp. 132 – 144, 2010.
- [4] Stephan Preibisch, Stephan Saalfeld, and Pavel Tomancak, "Globally optimal stitching of tiled 3d microscopic image acquisitions," *Bioinformatics*, vol. 25, no. 11, pp. 1463–1465, 2009.
- [5] B.S. Reddy and B.N. Chatterji, "An fft-based technique for translation, rotation, and scale-invariant image registration," *Image Processing, IEEE Transactions on*, vol. 5, no. 8, pp. 1266–1271, aug 1996.
- [6] Y. Keller, A. Averbuch, and M. Israeli, "Pseudopolar-based estimation of large translations, rotations, and scalings in images," *Image Processing, IEEE Transactions on*, vol. 14, no. 1, pp. 12–22, jan. 2005.
- [7] Rafael C. Gonzalez and Richard E. Woods, *Digital Image Processing*, Addison-Wesley Longman Publishing Co., Inc., Boston, MA, USA, 2nd edition, 2001.
- [8] K. Liu, Q. Wang, W. Driever, and O. Ronneberger, "2d/3d rotation-invariant detection using equivariant filters and kernel weighted mapping," in *IEEE Conference on Computer Vision and Pattern Recognition (CVPR)*, 2012.
- [9] P. Thevenaz, U.E. Ruttimann, and M. Unser, "A pyramid approach to subpixel registration based on intensity," *Image Processing, IEEE Transactions on*, vol. 7, no. 1, pp. 27–41, jan 1998.
- [10] L. Hogrebe, A.R.C. Paiva, E. Jurrus, C. Christensen, M. Bridge, JR Korenberg, and T. Tasdizen, "Trace driven registration of neuron confocal microscopy stacks," in *Biomedical Imaging: From Nano to Macro, 2011 IEEE International Symposium on*. IEEE, 2011, pp. 1345–1348.